

Stress and Strain Profiles along the Cross-Section of Waste Tire Rubberized Concrete Plates for Airport Pavements

E. Ferretti¹ and M.C. Bignozzi²

Abstract: In this study, the results of an in-situ experimental program on the performance of concrete taxiways are presented. The experimental program has been undertaken at the Guglielmo Marconi airport of Bologna (Italy). It concerns two portions of the taxiway, one built with plain concrete and one with rubberized concrete. Each portion has been instrumented with strain gauges embedded in concrete for the acquisition of vertical strains. The results of the experimentation are discussed in view of possible applications to the computational analysis of the stress field induced into pavements by aircrafts.

Keywords: Waste tire rubberized concrete, Elastic half-space, Environmental pollution.

1 Introduction

Rubberized concrete is obtained by replacing a part of the fine or coarse aggregate with rubber scraps. This produces a concrete with low unit weight, high toughness, high impact resistance and increased deformability or ductility.

One of the most interesting rubberization techniques of concrete, as far as the recycling of waste materials is concerned, is the use of grinded discarded tires. Actually, waste tires are a major concern among waste materials, as they can no longer be dumped in landfills and the amount of waste tires is constantly increasing due to the growing demand for tires and because of their short lifetime. Consequently, the only way to dispose of tires is to recycle them.

Waste tires have hardness and elasticity properties superior to those of rubber. Moreover, they can be used in almost any environmental condition and in any climate due to their good resistance to weathering, anti-caustic and anti-rot properties.

¹ DICAM, Facoltà di Ingegneria, Alma Mater Studiorum, Università di Bologna, Viale Risorgimento 2, 40136 (BO), Italy.

² DICAM, Facoltà di Ingegneria, Alma Mater Studiorum, Università di Bologna, Via Terracini 28, 40131 (BO), Italy.

In the last 20 years, several researchers have investigated the changes of strength, workability and dynamic characteristics of rubberized concretes in terms of size and amount of rubber scraps and rubber types [Topçu (1995); Fattuhi and Clark (1996); Fedroff, Ahmad, and Savas (1996); Khatib and Bayomy (1999); Wang, Wu, and Li (2000); Hernandez-Olivares, Barluenga, Bollatib, and Witoszek (2002); Li, Stubblefield, Gregory, Eggers, Abadie, and Huang (2004); Naik and Siddique (2004); Yang, Kim, Lee, Kim, Jeon, and Kang (2004); Ghaly and Cahill IV (2005); Bignozzi and Sandrolini (2006); Zheng, Sharon Huo, and Yuan (2008); Topçu and Sarıdemir (2008)]. It was found that rubberized concrete is an ideal material for all those structural members which are subjected to the immediate effects of impact and for which desired deformability or toughness is more important than strength, such as jersey barriers, road foundations and bridge barriers. In particular, rubberized concrete was shown to be capable of absorbing impact energy and reduce or minimize vibration more efficiently than traditional concrete.

As far as the constitutive behavior of rubberized concrete is concerned, some similarities can be established between the decrement in strength and stiffness of rubberized and fiber reinforced concrete, with the decrement being higher for higher amounts of rubber scraps. Thus, it seems reasonable that the micromechanics-based models developed for fiber reinforced concrete [Pahr and Böhm (2008); Kwon and Lee (2009); Lee, Kim, Kim and Kim (2009); Pyo and Lee (2009); Lee, Lee, Kim and Kim (2010)] could be easily adapted to rubberized concrete.

Since a material with high plastic energy could show higher deformation at the time of fracture and absorb more energy, with the plastic energy capacities enhanced, the idea underlying this investigation is that rubberized concrete may be used in airport pavements, in order to delay cracking and increase the skid resistance of concrete runways and taxiways. By absorbing impact energy, this material may also prevent possible damages to aircraft undercarriages during landing.

2 Airport pavements

An airport pavement is a structure consisting of one or more layers placed on a prepared subgrade. Pavements must be designed in such a way that they can bear the loads imposed by aircraft, whether they are indoor (hangar floors) or outdoor loads. A pavement must be smooth and stable under loading conditions during its expected or economic life. It must be capable of spreading and transmitting an aircraft weight to the existing subsoil (or subgrade) in a manner that precludes subsoil failure. Another function of the pavement is to prevent the weakening of the subsoil by moisture intrusion, especially from rainfall and frost.

There are a number of factors that affect the capacity of a pavement to ensure satis-

factory service: the quality of the pavement foundation (sub-grade), the magnitude and character of the aircraft loads to be carried, the traffic volume, which means load repetition, the concentration of traffic in certain areas, the quality of the materials used in construction and the climatological conditions. The main cause of the alteration of the physical properties of pavements over time is a combination of environmental conditions, aircraft loadings, mix design, materials and construction workmanship. Pavement performances are especially sensitive to the frequency of loadings. Areas subjected to repeated loadings due to concentration of traffic must be designed to accommodate the stresses arising from such loadings. The repetition of load by heavy vehicles will contribute to cumulative damage over the life of the pavement. The repetition is much smaller on airport runways and taxiways than highways, but the involved weights are greater for airport pavements. The major distresses on airfield pavements are caused by slow moving loads on the taxiways and ends of runways, where traffic follows a designated line. The ends of the runway are also involved by static load conditions coupled with vibration, due to running up the engines of jet aircraft to develop full thrust. This imposes high stress concentrations in the pavement. Little distress is generally found on the aprons or in the center portion of the runways.

Not all the movements of an aircraft, like takeoff and landing, take place in the same position. The position of landing, for example, is influenced by the pilot's accuracy, cross wind, width of runway, etc. This phenomenon is called lateral wander and is normally simplified by dividing all movements into a normal distribution around the centerline marking on the pavement. Lateral wander has an important influence on the rutting performance of pavements (Fig. 1), since individual aircraft wander patterns create traffic lanes.

Three basic approaches are in use in the United States to account for traffic wander [Yoder and Witczak (1975)]: the Asphalt Institute Method, the Portland Cement Association Method and the Corps of Engineers Method. In the third method, the lateral distribution of traffic is assumed to be uniform within a certain design Traffic Lane, in contrast to a normal distribution. All the methods agree in assessing to taxiways a traffic channelization degree higher than that of runways. The traffic is highly channelized also on runway ends and turnoff areas from the runway to the taxiway or to the apron area.

The wander width is defined by the zone containing 75% of the aircraft centrelines (1.15 standard deviations on either side of the mean value with a normal distribution). Data collected in the 1970's indicate wander widths of 1778 mm for taxiways and 3556 mm for runways. The standard deviation was found as 775 mm for a taxiway and 1524 mm for a runway [Ho Sang (1975)].

It is not only individual aircraft wander that affects pavement performance. Air-

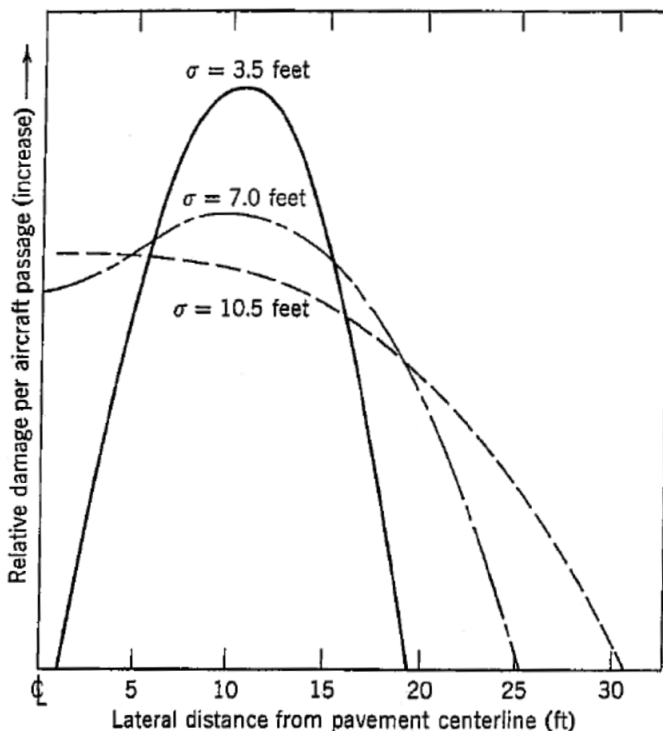


Figure 1: Effect of standard deviation σ of aircraft wander on pavement damage

crafts can have two or more landing gears at different positions from the body of the aircraft. Due to different gear assemblies (Fig. 2), the critical positions are not equally loaded by all aircrafts. Different aircraft combinations will induce additional wander that is not associated with lateral deviation of individual aircraft. Full scale pavement testing of aircraft loads at the FAA's National Airport Pavement Test Facility (NAPTF) indicate that wander can negate the stiffening in unbound granular layers (the shakedown effect), and make them prone to increased deformations on subsequent aircraft passes.

The size and number of airplanes, as well as the introduction of large and heavy aircrafts and changes in wheel loads and tire pressures, significantly affect pavement performance. Finally, in cases where the pavement is particularly rough, it can accelerate aircraft fatigue from both the dynamic response of the aircraft and accelerated loading on the pavement.

Taking into account the type, frequency and lateral wander of the carrying load, airfield pavements are divided into critical areas, where the aircraft speed is low or

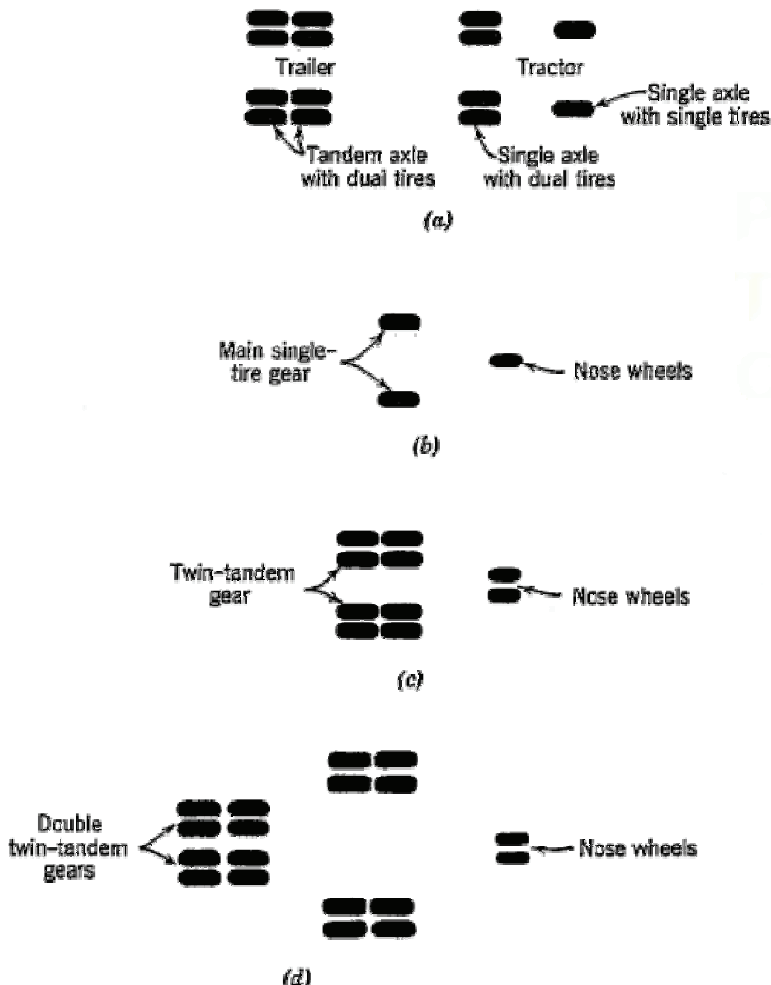


Figure 2: Plan view of basic types of wheel configuration: a) single trailer-truck unit; b) tricycle landing gear with single tires; c) twin-tandem landing gear; d) double twin-tandem landing gear (not to scale)

the aircraft is at rest (aprons, hard standings, taxiways, runway ends, turnoff ramp and hangar floors) and noncritical areas, where the aircraft speed is high or the aircraft is already partially airborne (central portions of runways and high-speed exit taxiways). Touchdown at the end of the runway may not be critical because the airplane is partially airborne. The condition of takeoff governs thickness design of airport pavements since under this condition the load is greatest due to fuel weight.

Different ranges of safety factors are recommended for critical and noncritical areas: 1.7-2.0 for critical areas and 1.4-1.7 for noncritical areas [Packard (1973)]. The distance from the end of the runway for which a thickened section is used ranges between 10% of the total runway length and 1000 feet. For major airports serving large volumes of traffic, the central portion of runways may be considered a critical traffic area. Since a greater safety factor for the central portion of the runway is appropriate in this case, leading to a greater runway thickness, designers sometimes select a keel-section design where the centre section of the pavement is thicker than the outside pavement edges.

On the basis of either lateral traffic distribution or aircraft weight or both, the airfield areas are also divided into four so-called traffic areas (Fig. 3), which attempt at categorizing common areas of distress, with the concentration of maximum loaded aircrafts decreasing from area A to D.

Type A traffic areas are the pavement facilities that receive the channelized traffic and full design weight of aircraft (taxiways, aprons through taxiways, the first 500 foot ends of runways). Aircraft with steerable gear, including fighter-type aircraft, operate within a relatively narrow taxilane producing sufficient coverages or stress repetition within the narrow lane to require special design treatment. These traffic areas require a greater pavement thickness than those where traffic is more evenly distributed.

Type B traffic areas are those in which traffic is more evenly distributed over the full width of the pavement facility, but which receive the full design weight of the aircraft during traffic operations (the second 500 foot ends of runways, aprons, parking, aircraft maintenance pavements for all heavy multiple-wheel aircraft). The repetition of stress within any specific area is less than on Type A traffic areas; therefore, a reduction in required pavement thickness can be allowed.

Type C traffic areas are those in which the volume of traffic is low or the applied weight of the operating aircraft is generally less than the design weight (runway interior, secondary taxiways, calibration hardstands). All runway interiors, except shortfield, will be designated as Type C traffic areas, since there is enough lift on the wings of the aircraft at the speed at which the aircraft passes over the pavements to reduce the stresses applied to the pavements considerably. Thus, the pavement thickness can be reduced in these portions of the runways. For the heavy, modified heavy, and medium-load airfields, the edges of the runway seldom receive a fully loaded aircraft; therefore, for these airfields, Type C traffic areas are limited to the central 23-meter (75-foot) width of runway interior. However, in seasonal frost areas, it may be necessary to use a uniform thickness for the entire width of the runway to preclude frost heave.

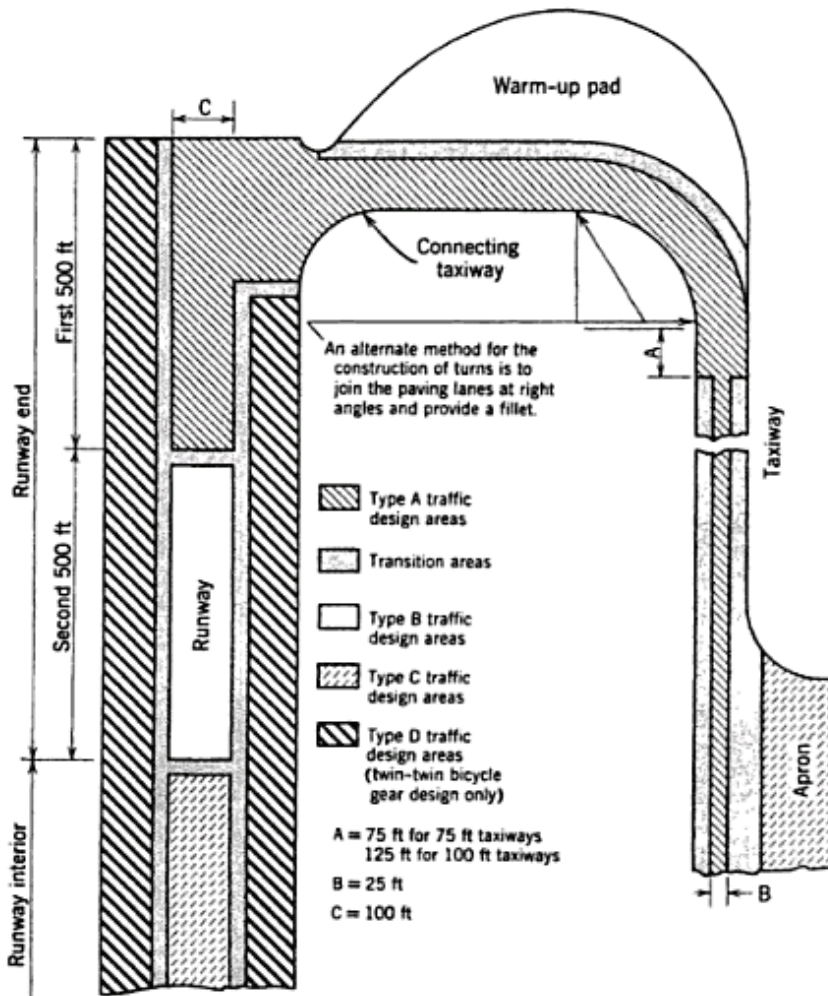


Figure 3: Traffic areas for heavy-load pavements based upon the Corps of Engineers design for all military (Army and Air Force) pavements

Type D traffic areas are those in which the traffic volume is extremely low and/or the applied weight of operating aircraft is considerably lower than the design weight (the outside 100 foot width in each runway side). The pavement facilities considered to be Type D traffic areas are the edges of runways that are designed for heavy-load, medium-load, and modified heavy-load airfields. Aircrafts on heavy-, modified heavy-, or medium-load runways seldom, if ever, operate outside of the central 23-meter (75-foot) width of the runway interior, and the only traffic that

will occur on the edges of the runway will be occasional heavy, medium, or modified heavy aircraft loads or frequent light aircraft loads. Therefore, a substantial reduction in required pavement thickness can be made.

The failure of an airfield pavement can be a structural rather than a functional failure. The first type of failure includes a collapse of the pavement structure or a breakdown of one or more of the pavement components of such a magnitude as to prevent the pavement from supporting the loads imposed upon its surface. The second type of failure may or may not be accompanied by structural failure, but is such that the pavement will not carry out its intended function without causing discomfort to passengers or without causing high stresses in the plane that passes over it, due to its roughness. Overload, including excessive gross loads, high load repetitions, and high tire pressures can cause either structural or functional failure. Climatic conditions as well as environmental conditions may cause surface irregularities and structural weaknesses to develop: frost heaving, volume change of soil due to wetting and drying, breakup resulting from freezing and thawing, or improper drainage may be the prime causes of pavement distress. A further cause of distress may be the disintegration of the paving materials due to freezing and thawing and/or wetting and drying. Base-course materials may breakdown, thus generating fines which may cause an unstable mix to develop. Subgrades also are susceptible to climatic conditions. Also construction practices may have some effect: rutting of the subgrade during construction allows water to accumulate and subsequently soften the subgrade when the construction has been completed, and the use of dirty aggregates may cause pavement deterioration [Yoder and Witczak (1975)].

Sealing of cracks and joints at appropriate time intervals will ensure a tight wearing surface, as a measure against surface infiltration of water.

There are two types of airfield pavements, rigid and flexible pavements. The basis for classification is the way by which wheel loads are transmitted to the subgrade soil through the pavement structure (Figs. 4, 9). Moreover, in flexible pavements the total pavement structure deflects, or flexes, under loading, while it deflects very little under loading in rigid pavements.

2.1 Flexible pavements

Flexible airfield pavement is a structure composed of several layers of material placed on a subgrade, each of which receives the loads from the above layer, spreads and distributes them out over a wider area (Fig. 4), then passes them on the layer below [Wei (2009)]. Since the loaded area increases with depth, the further down in the pavement structure the layer is, the fewer loads it must carry. The pavement structure is designed to take advantage of the decreasing magnitude of

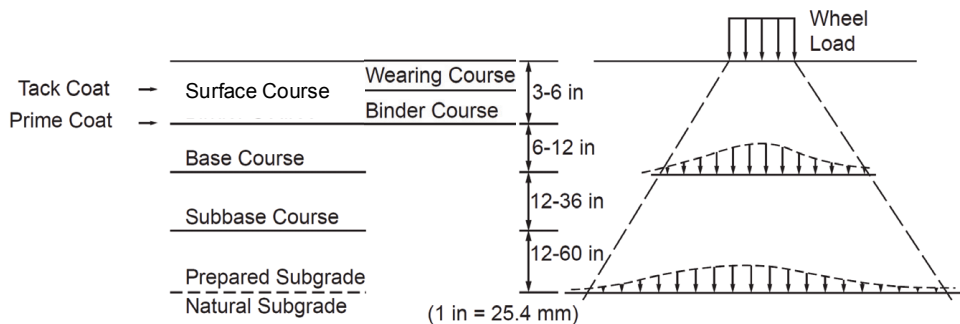


Figure 4: Typical cross section and stress transmission in flexible pavement

stresses with depth. It has a total thickness, so that the stresses and strains in the subgrade soil layers are within the required limits. The strength of subgrade soil is expected to directly affect the total thickness of the flexible pavement. Moreover, the stresses induced on a given subgrade material can be decreased by increasing the thickness of the overlying layers.

Material layers are usually arranged in order of descending load bearing capacity with the highest load bearing capacity material (and most expensive) on the top and the lowest load bearing capacity material (and least expensive) on the bottom.

Flexible airport pavement typically consists of four layers (Fig. 4):

- Bituminous surface course;
- Base course;
- Subbase course;
- Subgrade course.

All the layers are important to pavement strength, as well as drainage and frost protection.

The surface course provides characteristics such as friction, smoothness, noise control, rut and shoving resistance and drainage. In addition, it has the purpose of preventing the introduction of excessive quantities of surface water into the underlying base, subbase and subgrade. It usually consists of two layers: the wearing course, at the top, and the binder course, at the bottom. The wearing course is meant to take the brunt of traffic wear and can be removed and replaced as it becomes worn. The binder course is meant to distribute load. A light application of tack coat of

water-diluted asphalt emulsion may be used to enhance bonding between the two courses (Fig. 4).

Base courses are most typically constructed from durable aggregates, either stabilized or unstabilized, or successive layers of crushed rock mechanically locked by rolling and bonded by stone screening (Macadam Base), or crushed stones laid, shaped and compacted and then added to finer materials and washed into surface to provide a dense material (in-water bound Macadam), or, finally, mineral aggregate and additive to make them strong or more resistant to moisture (Treated Bases). The materials should be dense and uniformly graded so that no differential settlement occurs and must be capable of being compacted. Base courses of untreated natural materials are less affected by adverse weather and normally require less technical control. Untreated bases are relatively easy and fast to build and are preferable to bituminous or cement-stabilized types.

The subbase is a structural support that also minimizes the intrusion of fines from the subgrade into the pavement structure and minimizes frost action damage. It also prevents the subgrade and base from being mixed up. The subbase course may be omitted when the subgrade is stiff and of high quality. If this is not the case, the subbase may consist of high quality fill used to replace poor quality subgrade. The subgrade material should be clean and free from organic matter and should be able to be compacted by roller to form a stable sub-base.

The subgrade shall be compacted to a minimum 95% density and stable to prevent rutting and shoving during construction, provide support for the placement and compaction of paving lifts, limit pavement resilient deflections and rutting of the subgrade during the service life of the pavement. Any distortion or displacement occurring in the subgrade is reflected in the subbase course and continues upward into the base and surface courses.

It is worth noting that, even if classified as flexible pavements, asphalt pavements may possess the same stiffness as Portland cement concrete pavements, which are classified as rigid pavements, when stabilized materials are used in any of the pavement components. The same is true when relatively thick asphaltic concrete layers are used. Hence, the definitions of flexible and rigid pavement may or may not be strictly true. They were originally established in the unique attempt to distinguish between asphalt and Portland cement concrete pavements, respectively, and do not strictly rely to stiffness. As a consequence, if an asphalt pavement has high stiffness, fatigue of the surface or of any pavement components may become critical as it happens in rigid pavements. In these cases, concepts underlying design approach those historically adopted for concrete pavement design [Yoder and Witczak (1975)].

The use of flexible pavements on airfields must be limited to those pavement areas not subjected to detrimental effects of fuel spillage, severe jet blast, or parked aircraft. Actually, fuel spillage leaches out the asphalt cement in asphaltic pavements and jet blast damages bituminous pavements when the intense heat is allowed to impinge in one area long enough to burn or soften the bitumen, so that the blast erodes the pavement. Flexible pavements are generally satisfactory for runway interiors, secondary taxiways, shoulders, paved portions of overruns, or other areas not specifically required to have a rigid pavement surfacing. These areas coincide with the noncritical areas, previously defined (§ 2). In conclusion, flexible pavements should be possibly avoided in critical areas.

There are four major categories of common asphalt pavement surface distresses [Bennet (2004)]: surface defects (raveling, flushing, and polishing), surface deformation (rutting and distortion, such as rippling and shoving, settling, frost heave), cracks (thermal, reflection, slippage, joint/edge, block, and alligator cracks), patches and potholes.

As far as surface deformation and cracks are concerned, rutting is the displacement of material that creates channels in wheelpaths. It is caused by traffic compaction or displacement of unstable material. Shoving or rippling is the displacement of surfacing material. It can develop when the asphalt mixture is unstable because of poor quality aggregate or improper mix design. In general, surface deformation may hinder rain drainage, causing hydroplaning when one or more tires loose contact with the surface as a result of the buildup of water pressure in the tire-ground contact area. The potential for hydroplaning is a function of speed, water depth, pavement texture, tire inflation pressure, and tread design.

Thermal cracks are often regularly spaced. The cause is movement due to temperature changes and hardening of the asphalt with aging. Differential thermal stress can also cause cracking. Pavement marking paint and sealcoats using materials with significantly different thermal properties can create surface cracking.

Reflection cracks are cracks in overlays which reflect the crack pattern in the pavement underneath. They are caused by movement in the underlying pavement due to temperature change. This movement creates very large stress in the overlay.

Slippage cracks are crescent or rounded cracks caused by slippage between an overlay and an underlying pavement. Slippage is most likely to occur at locations where traffic is stopping and starting.

Paving joint cracks are caused by inadequate bonding and poor compaction of the joint during construction. They may also be caused by reflection of poor joints in the underlying pavement.

Block cracking is interconnected cracks forming large blocks. Cracks usually in-

tersect at nearly right angles.

Alligator cracks are interconnected cracks forming small pieces. This is caused by failure of the entire pavement due to traffic loading (fatigue) and usually due to inadequate base or subgrade support.

Some examples of distresses occurred on the flexible taxiway of the Guglielmo Marconi Airport are shown in Figs. 5–8.



Figure 5: Rutting and alligator cracks near the centerline



Figure 6: Behavior of the taxiway after a rain: the undrained water staying inside the wheelpaths channels created by rutting, possible cause of hydroplaning, is well evident; wheelpath cracking caused by traffic loads is also evident in the upper left corner

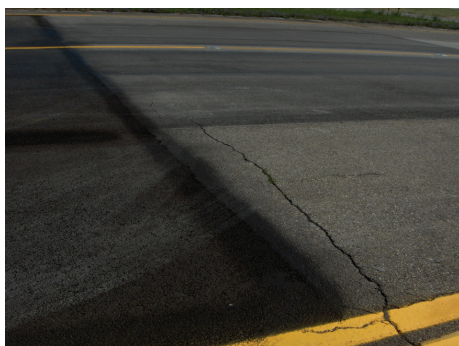


Figure 7: Open cracks with some grass growing inside



Figure 8: Detail of Fig. 7 and polished worn aggregates on the taxiway surface

Water flow can also affect the durability of asphalt mixtures. A discussion on how moisture can infiltrate into the composite structure of asphalt mixtures and adversely affect its mechanical performance, causing the separation of the aggregates from the wearing surface (raveling and stripping), can be found in Kringos, Scarpas and Selvadurai (2008).

The intensity of stress at a given point in a flexible pavement is affected by the tire-contact area and tire pressure. The major difference in stress intensities caused by variation in tire pressure occurs near the surface. Consequently, the surface course and base course are the most seriously affected by high tire pressures.

2.2 Rigid pavements

Rigid airport pavement consists of a slab of Portland cement concrete (PCC) that rests on a subgrade or subbase. Rigid pavements carry traffic loadings differently than flexible pavements (asphalt). A major part of the load-carrying capacity is derived from the beam action of the slab. The major factor considered in the design of rigid pavements is the structural strength of concrete. For this reason, variations in the modulus of elasticity and Poisson's ratio of the subgrade have only a slight effect on the thickness design and structural capacity of the pavement.

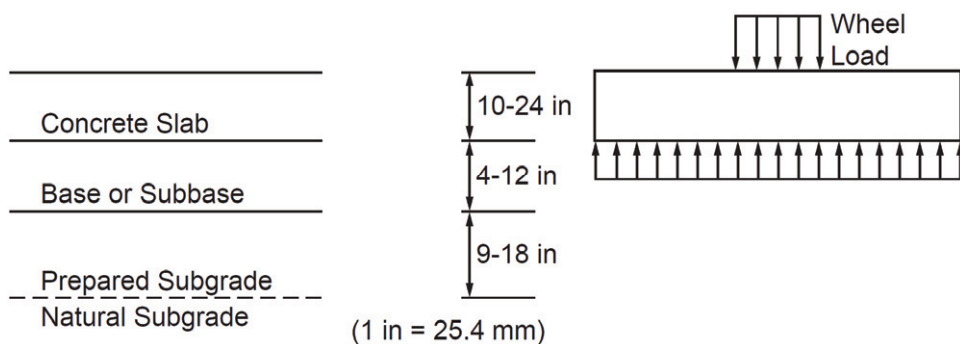


Figure 9: Typical cross section and stress transmission in rigid pavement

Because of the rigidity of concrete pavements, loads are spread over the entire slab area (Fig. 9) and pressures on the subgrade are very low. As a result, concrete pavements do not necessarily require strong support from below. However, it is important that the support be reasonably uniform with no abrupt changes in degree of support.

The surface course is the stiffest and provides the majority of strength. It also provides characteristics such as friction, smoothness, noise control and drainage. In

addition, it serves as a waterproofing layer to the underlying layers. The surface course can vary in thickness but is usually between 150 mm (6 inches) (for light loading) and 300 mm (12 inches) (for heavy loads and high traffic). Its strength allows it to bridge over minor irregularities that may occur in the base or the subgrade upon which it rests.

The underlying layers are less stiff orders of magnitude, but still contribute importantly to pavement strength, as well as drainage and frost protection.

Base courses uniformly support the pavement and also help prevent subgrade soil movement due to slab pumping and shrink and swell of the subgrade itself. They are usually constructed out of a simple base course of crushed aggregate or stabilized aggregate or soil, dense-graded HMA (where high base stiffness is desired), open graded permeable HMA (where high base stiffness and excellent drainage is desired) and, finally, lean concrete.

The subbase course is a structural support that also minimizes the intrusion of fines from the subgrade into the pavement structure and minimizes frost action damage. It generally consists of lower quality materials than the base course but better than the subgrade soils. Appropriate materials are aggregate and high quality structural fill. A subbase course is not always needed or used.

The three major causes of non-uniform support are expansive soil, frost action and mud-pumping [Packard (1973)]. Effective control of expansive soils and frost action is achieved through appropriate subgrade preparation techniques, while prevention of mud-pumping requires a granular or stabilized subbase layer.

Relatively thin subbases may be placed under rigid pavements to prevent pumping and also improve a low strength subgrade. Cement-treated subbases offer many benefits in addition to the prevention of mud-pumping [Packard (1973)].

Due to its higher stiffness, the rigid pavement is recommended in critical areas, where the danger of distress is higher since the traffic is highly channelized (taxiways) and/or live loads concentrate over longer periods of time (apron and associated service road), in order to avoid wheel ruts due to repeated tracking of aircraft and equipment. On the aprons and at runway ends, where aircrafts stand, the use of concrete pavements is to be preferred to asphalt ones also because fuel spillage is frequent in those areas and the asphaltic concrete is vulnerable to damage by aviation fuel. The list of the rigid pavements includes all paved areas on which aircrafts or helicopters are regularly parked, maintained, serviced, or pre-flight checked; hangar floors and access aprons; runway ends (305 meters (1,000 feet)) of a Class B runway; areas that may be used from the runway end to 90 meters (300 feet) past the barrier to control hook skip; primary taxiways for Class B runways; hazardous cargo, power check, compass calibration, warmup, alert,

arm/disarm, holding, and washrack pads; and any other area where flexible pavements can be proved to be susceptible to damage by jet blast or spillage of fuel or hydraulic fluid. The 2 meters (6.56 feet) of pavement on both the departure sides of the arresting gear pendent shall be PCC for Navy and Marine Corps. Rigid pavements shall also be used at pavement intersections where aircrafts/vehicles have a history of distorting flexible pavements and where sustained operations of aircrafts/vehicles with tire pressures in excess of 2.06 MPa (300 psi) occur. Finally, continuously reinforced concrete pavement will be used in liquid oxygen (LOX) storage and handling areas to eliminate the use of any organic materials (joint sealers, asphalt pavement, etc.) in those areas.

The stress produced in rigid pavements can be related to:

- Curling stresses due to temperature differential through the thickness of the slab and warping stresses to difference in moisture;
- Frictional stresses due to uniform temperature variations;
- Infiltration stresses resulting from the filtering down of foreign matter into the joint, or from pumping action where the sub-grade material is forced up into the joint by the jetting action o pumping water;
- Load stresses due to externally applied loads.

In areas where freezing conditions exist, the pavement should be built of air-entrained concrete.

PCC pavements are either plain (non-reinforced) or reinforced concrete. Reinforcement is usually provided by a steel wire mesh placed approximately at mid-slab depth. The reinforcement is intended to limit crack opening and movement in the concrete slab. Since concrete slabs need to move expand and contract with changes in temperature and during initial cure (drying and shrinkage), pavements are constructed with contraction joints. This joint gives the slab a place to crack and makes a straight, well-formed groove to seal.

Since concrete pavements are designed to act like a beam and use the bending strength of the slabs to carry the load, load transfer across cracks and joints is important, especially on pavements with heavy traffic loading. Many concrete pavements use joints that have load transfer dowels. These are smooth steel bars placed across the joint. They transfer traffic loads between adjacent concrete slabs, while allowing the joint to open and close. These bars can rust and sometimes cause problems. The corrosion causes forces on the concrete which leads to spalling, cracking, and general joint deterioration. Unsupported slab edges will deflect or bend under a load.

If the supporting soil is saturated, it can squirt up through joints or cracks when the slab bends. This is called pumping. Eventually the loss of supporting soil through pumping creates an empty space or void under the slab. The slabs may then crack further under loads and joints will deteriorate more.

Undoweled joints under heavy traffic may fault. This is when one slab edge is lower than the next slab. Faulting is more likely on pavements with most of the traffic in one direction. The downstream traffic slab will be lower than the upstream slab, creating a step. Faulting creates a rough pavement.

There are four major categories of common PCC pavement distresses [Bennet (2004)]: surface defects (polishing, map cracking, pop-outs, scaling, spalling), joints (longitudinal and transverse joints), pavement cracks (slab cracks, D-cracking, corner cracks, meander cracks, manhole and inlet cracking), pavement distortion (pavement settlement or heave; blow ups; faulting; utility repairs, patches and potholes). In particular, a pattern of fine cracks usually spaced within several inches is called map cracking. It usually develops into square or other geometrical patterns. Map cracking can be caused by improper cure or overworking the surface during finishing. It may also indicate a problem with the quality of the aggregate known as ASR (alkali-silica reactivity).

Individual pieces of large aggregate may pop out of the surface. This is often caused by chert or other absorbent aggregates that deteriorate under freeze-thaw conditions. Pop-outs alone do not usually affect pavement serviceability. However, damage to aircraft from the debris may occur.

Scaling is surface deterioration that causes loss of fine aggregate and mortar. More extensive scaling can result in loss of large aggregate. The cause is often the use of concrete that has not been air-entrained, thus making the surface susceptible to freeze-thaw damage.

Spalling is the loss of a piece of the concrete pavement from the surface or along the edges of cracks and joints. Cracking or freeze-thaw action may break the concrete loose, or spalling may be caused by poor quality materials. As pavements age and materials deteriorate, joints may open wider and deteriorate further. Cracks parallel to the initial joint may develop and accelerate into spalling or raveling.

Settlement, instability, or pumping of subgrade soil can cause joints to fault. One common cause of cracks parallel to joints is waiting too long after the pour to saw the joint. Then, during initial cure the slab will crack near the sawn joint. Slab cracks divide the slab into 2 or more pieces. They can be caused by thermal stresses, poor subgrade support, or heavy loadings. They are sometimes related to slabs with joints spaced too widely. Occasionally, severe deterioration may develop from poor quality aggregate.

The so-called D-cracks or disintegration cracking develop when the aggregate absorbs moisture. This causes the aggregate to break apart under freeze-thaw action, which leads to deterioration. Usually, it starts at the bottom of the slab and moves upward. Fine cracking and a dark discoloration adjacent to the joint often indicate a D-cracking problem.

Diagonal cracks may develop near the corner of a concrete slab, forming a triangle with the joint. Usually these cracks are within a foot or two of the slab corner and are caused by insufficient soil support or concentrated stress due to temperature-related slab movement. The corner breaks under traffic loading.

Some pavement cracks appear to wander randomly. They may cross a slab diagonally or meander in a random manner. Meander cracks may be caused by settlement due to unstable subsoil or drainage problems. Frost heave and spring thaw can also cause them. They are often local in nature and may not indicate general pavement problems.

Concrete slabs may push up or be crushed at a joint. This is caused by the expansion of the concrete where incompressible materials (sand, debris, etc.) have infiltrated into poorly sealed joints. As a result, there is no space to accommodate the expansion.

2.3 State of the art of the models for analytical design

The paving of airport runways, taxiways, and aprons has provided a strong market for Portland cement concrete in recent years, as commercial and military airports upgrade their ground facilities to keep up with increasing air traffic. Concrete provides the substantial pavement strength required to withstand the impact of airplanes such as the 747, which can weigh more than 850,000 *lb* (382,000 *kg*) when fully loaded.

The first United States airport runway was built in 1928 in Dearborn, Michigan, by the Ford Motor Company for a Ford-manufactured plane called the Silver Goose. This and other early runways used variable pavement thicknesses similar to those of early highways: concrete 8 or 9 *in.* (20 or 22.5 *cm*) deep at the edges and 6 or 7 *in.* (15 or 17.5 *cm*) thick at the center. Until World War II, engineers designed these concrete pavements based on the anticipated loads imposed by refueling trucks carrying gasoline to the airplanes, rather than the airplanes themselves, because the trucks imposed a more critical wheel load. Concrete pavement markets span from driveways and parking lots to mainline interstate highways.

In 1942, at the beginning of World War II, 93 million *sq yd.* (74 million *sq m*) of airfield pavement was placed in the United States as the country mobilized to get planes airborne. At that time, 6 *in.* (15 *cm*) deep concrete pavements were the

norm, but heavier airplanes created the need to increase concrete runway pavement depth to 12 in. (30 cm) thick. Eventually, engineers specified runway pavements as thick as 24 in. (60 cm) to accommodate heavy loads imposed by larger aircraft. The addition of more wheels to these airplanes, which better distributed the loads on the pavement, reduced the pavement depth required to 12 in. (30 cm) in the late 1940s.

Today, specifications for airport concrete pavement vary depending on subgrade conditions, expected loading, and anticipated pavement life-span. New concrete runways at non-hub airports generally range in thickness from 9 to 12 in. (22.5 to 30 cm), while runways at hub airports often are constructed 15 to 18 in. (37.5 to 45 cm) thick to withstand larger and more frequent loading.

For pavement design purposes, the maximum takeoff weights of the aircraft are usually considered. It is also common to assume that 95% of the gross weight is carried by the main landing gears and 5% by the nose gear.

Prior to the 1920s, all pavements were designed based on experience alone. The prediction of the propagation of the vertical stresses into the pavement and subsoil when carried by an aircraft, in particular, and a vertical load [Selvadurai and Ghiabi (2008); Pu, Zhihai, Xiasong, Guorong, Haili, Xiaoqin and Zhangzhi (2009); Manzanal, Pastor, Merodo and Mira (2010)], in general, is an open question still now. According to the type of traffic loads and climatic conditions, the type of damage concerned, the structure considered and the nature of the component materials, different types of response models can be used for airfield pavements.

All the stress models currently in use for flexible pavements design are directly or indirectly derived from Boussinesq's closed form solution for a homogeneous, linear-elastic and isotropic half-space subjected to a point-load perpendicular to the surface [Boussinesq (1885)]:

$$\sigma_v = \frac{3}{2} \frac{P}{\pi r^2} \cos^3 \theta, \quad (1)$$

where σ_v is the vertical stress at the distance r between the application and the evaluation points, θ is the angle between the point load vector and the radial arm connecting the application to the evaluation point and P is the point load applied at the surface (Fig. 10).

An analytical study of the linear-elastic problem for a continuously non-homogenous half-space can be found in Seyrafian, Gatmiri and Noorzad (2007).

From Eq. (1) it can be seen that the vertical stress of Boussinesq is dependent on the depth and radial distance and is independent of the properties of the transmitting medium. The distribution of radial stresses below a concentrated load on any horizontal plane takes the form of a bell-shaped surface (Fig. 11).

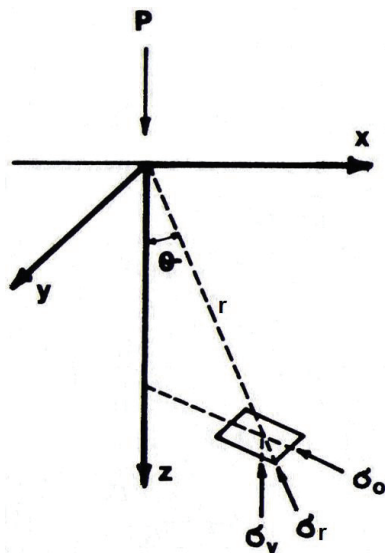


Figure 10: Parameter definition for Eq. (1)

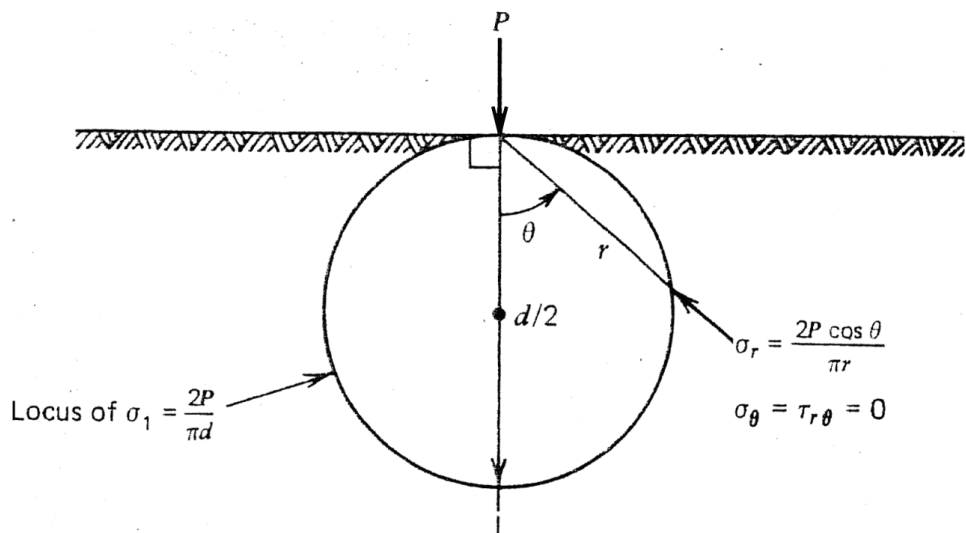


Figure 11: Radial stress distribution of Boussinesq in the semi-infinite linear-elastic medium below the wheel

Maximum stresses occur on the vertical plane passing through the point of load application. Variation of stress with depth for the more realistic case of load at the surface distributed over an elliptical tire-pavement contact area follows the same general pattern as for the point-load case.

Tests have shown that, for most cases, Boussinesq's equations result in stresses that are larger than measured values. Calculated deflections also tend to be greater than measured values.

Boussinesq was aware that Eq. (1) might not be valid for non-solid materials and had developed a theory for stresses in a granular medium, assuming the shear modulus to be proportional to the hydrostatic stress [Boussinesq (1876)]. Also Fröhlich's equation [Fröhlich (1934)] is an extension of Eq. (1) to the case of a granular medium:

$$\sigma_v = \frac{n}{2} \frac{P}{\pi r^2} \cos^n \theta, \quad (2)$$

where n is Fröhlich's stress concentration factor. It depends on the medium strength and modifies the distribution of the vertical stress in the half-space system, since Fröhlich showed that the vertical stress in granular media, in general, and in agricultural soils, in particular, was more concentrated around the point load vector than the stress predicted by Boussinesq's equation. The reason for this was assumed to be the elasto-plastic, and not fully elastic, behavior of the medium.

With $n = 3$ one obtains Boussinesq's equation. For values of n smaller than 3 Eq. (2) represents stress dispersion, while for values of n greater than 3 Eq. (2) represents a stress concentration. Higher concentration factors increase the depth at which the stresses propagate.

For a soil subjected to vehicular loading, Söehne (1958) assigns values to the concentration factors based on the soil properties: the concentration factor is 4 for hard soil, 5 for medium soil, and 6 for soft soil. However, Sharifat and Kushwaha (2000) suggest values of 3 for hard soil, 4 for normal soil, and 5 for soft soil. Binger and Wells (1989) suggested a method of determining the soil's concentration factor based on the soil density and its relationship to the maximum and minimum soil density.

It is worth noting that, unlike Boussinesq's equation which is the solution of a fourth-order differential equation, Fröhlich's equation is an empirical model only.

In 1973, Veverka showed that the conditions of equilibrium and compatibility required a variation of the elastic modulus with depth if Fröhlich's concentration factor differed from 3 [Veverka, (1973)]:

$$E = Cz^{\frac{n-1}{2}}, \quad (3)$$

where E is the elastic modulus, z is the depth and C is a constant.

For multi-wheel tire groups Eq. (2) takes the form:

$$\sigma_v = \sum_{i=1}^{wheels} n \frac{P_i}{2\pi r_i^2} \cos^n \theta_i, \quad (4)$$

in which the principle of superposition has been applied. Eq. (4) is the basis for the general case solution when computing the vertical stress in a half-space due to multi-wheel tire groups.

Several computer software have been developed for computing the vertical stress at the top of the subgrade due to a multi-wheel tire group, using numerical integration techniques of Eq. (4).

No closed form solutions, like Boussinesq's equations, exist for a layered system, like a pavement. The different approaches used to deal with layered elastic systems may be divided into:

- The Method of Equivalent Thicknesses (MET) [Odemark, (1949)], which transforms the layered system to semi-infinite halfspaces, on which Boussinesq's closed form solutions can be used;
- Layered Analytical Models (LAM) [Burmister (1943)], which are often referred to as mathematically exact solutions, where the fourth-order differential equation is solved for the given boundary conditions using numerical integration;
- Finite Element Models (FEM), which divide a continuum into smaller more manageable elements, finite in size, each of which has its material behavior defined. The behavior of each element can be analyzed separately and the cumulative deformations of the elements brought together to give a resulting deformation for the whole structure.

Stress and deflection values as obtained by Burmister are dependent upon the strength ratio of the layers. They are used to estimate development of pavement distress (rutting and fatigue cracking). Assuming the strength ratio equal to 1, it is possible to compare Burmister's analysis to that of Boussinesq: although at great depths the two analyses approach a common level, they are vastly different near the base-subgrade contact.

In 2000, the AMADEUS (Advanced Models for Analytical Design of European pavement Structures) consortium presented its final report for publication. The AMADEUS research project concerns the review and evaluation of pavement design models that are already in use for practical applications and for research projects.

The responses calculated by means of several design models or software packages were compared with measurements carried out on accelerated tests. It was found that vertical stress and strains are underestimated by up to 50% when compared to measured values with all models tested in AMADEUS. Predictions of deflection and horizontal strain are better with many teams reporting good or close agreement with their models. As pointed out in the AMADEUS final report, the systematic under estimation of vertical stress is an important finding that must be considered in further developments, since this stress component is indeed used in most pavement design methods as a criterion to avoid deformations and settlements of the subgrade. Its underestimation can thus result in early deterioration of the road structure. One of the conclusions of the study is that the elastic multi-layer theory can be used to obtain horizontal strains at the bottom of the asphalt layer. However, they are unable to model the vertical strains and stresses in the subgrade. On the contrary, although MET is not a precise method from a mathematical point of view, it can predict the strains and stresses in pavement layers reasonably well. Finally, Finite Element models require experienced users to be effectively applied. Also for this reason, they have not been formally developed for easy application.

In 1942, the CBR (California Bearing Ratio) method was adapted from the empirical road pavement design method to the design of flexible pavements to support heavy bombers [Gonzales (2006)] and is currently in use in the U.S. Military (Army, Air Force and Navy) as design procedure for both military roads and flexible airport pavements. The adaption utilizes Boussinesq's single elastic layer theory. The CBR procedure has been currently used throughout the world due to its simplicity and practicability. It is an empirical design method that relates the required pavement thickness for a prescribed number of load coverages to the CBR assigned to the subgrade under the pavement and the aircraft wheel load. It only considers stress, strain and deflection directly under a single wheel load. The major pavement failure mode is assumed to consist of surface rutting caused by shear failure of the subgrade, due to accumulated vertical deformations. The design procedure consists in increasing pavement thickness to protect the subgrade.

The classical CBR equation was developed from airfield design curves, obtained by modifying and verifying with extensive full scale field testing from the 1940s to the early 1970s the extrapolation, based on shear stress, of the California pavement design curves for highway pavements. The design curves are drawn specifically for each aircraft and the output data is the total thickness of the pavement above the layer to be protected. The traffic mixture is expressed in terms of a single design aircraft. All annual departures are converted to equivalent annual departures of the design aircraft. The aircraft wander is accounted for by means of the pass-to-coverage ratio (P/C), which is determined by statistical analysis of gear load

distribution at the pavement surface in the CBR method as implemented by the FAA and taken equal to 3.65 in the French CBR method.

The CBR-based design curves for flexible pavements were developed using the ESWL (equivalent single wheel load) concept for multiple-wheel gears. The ESWL is defined as the load on a single tire that produces the same maximum vertical deflection at surface or at pavement-subgrade interface (Fig. 12) as the multiple wheel load. The ESWL can also be defined as the load on a single tire that produces an equal magnitude of other preselected parameters at bottom face of bound layer, such as stress, strain, or distress.

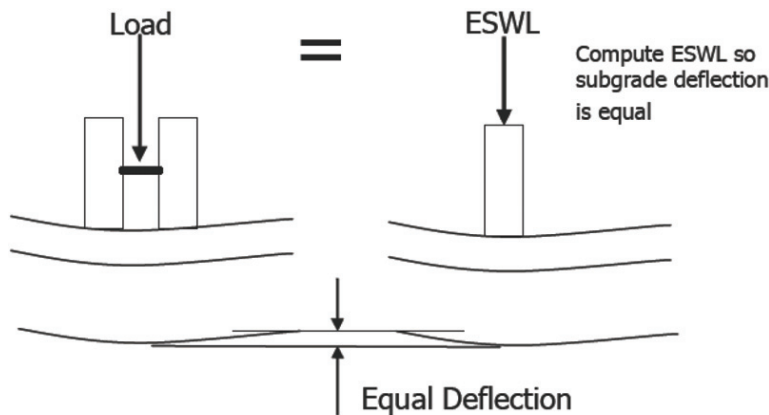


Figure 12: Equivalent single wheel load (ESWL) at subgrade level

For the ESWL calculation, the pavement structure is assumed to be a uniform elastic half-space (Boussinesq's model).

It has been shown [Barker and Gonzalez, 2006] that the current CBR criteria can be derived from Fröhlich's general solution for a stress concentration factor n equal to 2. This finding allowed for a reformulation of the classical CBR equation into a more general equation in terms of vertical stresses as computed with a stress concentration factor. Then, the algorithms and equations for a new CBR design procedure have been developed [Gonzales (2006)], providing thinner pavement sections for low subgrade CBR values and approximately equal to or slightly higher than the current procedure pavement thickness at higher CBR values.

The deficiencies of the CBR method in providing design thickness when alternative construction practices, new or innovative materials and ageing and seasonal effects are involved and providing the correct ESWL for multi-wheel landing gears are largely recognized today [Caron, Theillout and Brill (2010)]. As far as the last point is concerned, full-scale pavement tests to failure showed that the deflection-based

design procedure overpredicted the ESWL corresponding to multi-wheel landing gears, due to an over estimation of wheel interaction. Consequently, it was found that the damage caused by multiple wheel landing gear was less than that modeled under the ESWL. Some pavement thickness reduction factors, such as alpha (α) factors, were thus introduced in 1971 and used for many years in order to reduce the required pavement thickness for multiple-wheel aircrafts based on the number of wheels on the aircraft landing gear and the number of coverages to be designed for. However, this revised methodology was also shown to overstate the damaging effect of multi-wheel landing gears. Although some attempts have been made to adjust the CBR method, a gradual transition has taken place worldwide since the mid 1990s, abandoning the concept of design aircraft and moving to rational design concepts using mechanistic-based performance models and layered elastic procedures. However, the CBR method is still frequently used in airport pavement design.

The rational design methods used in both the US and France eliminate both the alpha factor and the need for ESWL calculations, since the contribution of each wheel in the gear assembly to the combined strain at the top of the subgrade is accounted separately by layered elastic analysis, and consist in verifying that a predesigned flexible structure can support mechanically over a particular subgrade a given level of traffic accumulated over a specified lifetime (20 years in the US and 10 years in France). Moreover, the pass-to-coverage ratio is computed at top of the subgrade, then adjusted by a factor between 1 and the number of wheels for tandem wheels, and the assumed wander is normally distributed with a standard deviation of 0.775 m in the US rational method, while the P/C concept is abandoned in the French rational method.

The main limitations of the rational method derive from the isotropic linear elastic theory that underlies this new design approach.

Rigid pavement thickness design is either still based on the classical Westergaard's solutions or on a more comprehensive finite element rigid pavement model to resolve the shortcomings of the layered elastic Burmister's model. Since the latter is time consuming, rigid pavements are often modeled as a Westergaard's slab even if the finite element model gives a better representation of the slab edge and joints. Westergaard's model [Westergaard (1943)] uses a dense liquid Winkler's foundation model. In general, Westergaard-Winkler's model overestimates the values of deflection and bending stress in a concrete slab. Some of the limitations of this model are slab size restriction, the inability to analyze the effects of load transfer efficiency across cracks and joints, and the inability to properly assess the effect of stabilized subbases on pavement behavior and performance.

Pasternak's foundation is an improvement of Westergaard-Winkler's model, achieved

by connecting horizontal springs to Winkler's springs.

3 Experimental set-up

The experimentation has been carried out on a 14 m length segment of the taxiway of the Guglielmo Marconi airport (Bologna, Italy), which is a 23 m wide flexible pavement taxiway (Fig. 13).

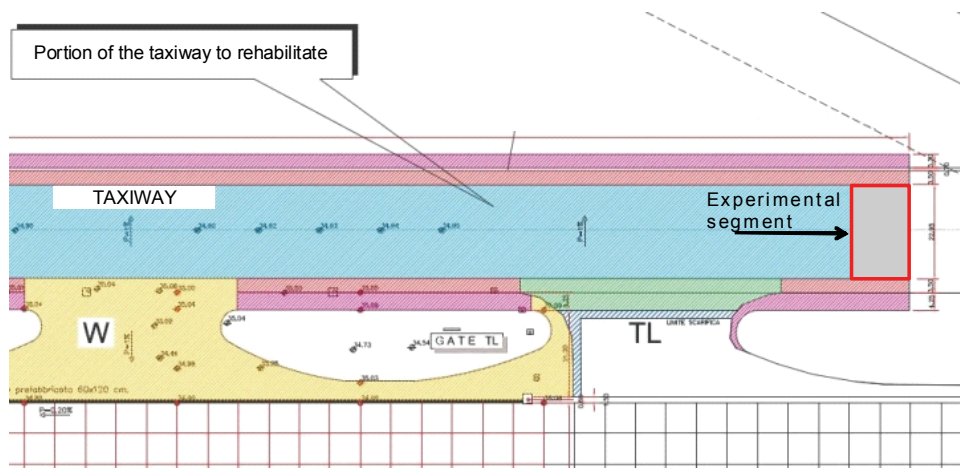


Figure 13: Detail of the rehabilitation interview, with $14 \times 23\text{m}$ the experimental segment boxed in red

A taxiway is a specially prepared or designated path on an airfield, other than apron areas, on which aircrafts move under their own power to and from landing, service, and parking areas (taxiing). Since planes have no motors for their wheels, the shear stresses arising in airfield pavements from the friction between the pavement and the aircraft wheels are opposite to those developed by cars. The involved friction is a rolling resistance friction. Actually, instead of pushing against the ground to produce its thrust, an airplane pushes against the air using a propeller or jet engine. By pushing air backwards, the plane pushes itself forwards in accordance with Newton's Third Law of Motion. The wheels are present not to provide a means of propulsion but to reduce the friction between the airplane and the ground, increasing net thrust.

The experimental segment was divided into two sections of 7 m each (Fig. 14), to be realized by substituting the base and binder courses of the flexible pavement with a slab of concrete. The reason for this choice lies in the fact that, as widely

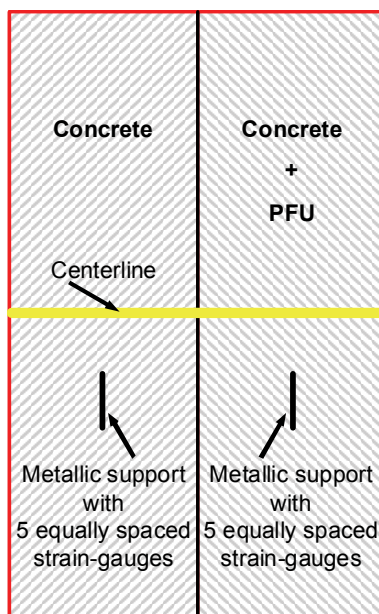


Figure 14: Detail of the experimental segment (boxed area in Fig. 13)

discussed previously (§2), the taxiway, being considered a critical area, should not be covered with flexible pavement.

Table 1: Cross-sections of the taxiway flexible and semi-rigid pavements.

Flexible pavement	Section 1 semi-rigid pavement	Section 2 semi-rigid pavement
Wearing course	4 cm	4 cm
Binder course	6 cm	/
Base course	10 cm	/
Plain concrete slab	/	16 cm
Rubberized concrete slab	/	16 cm
Subbase course	50 cm	50 cm
Subgrade course	30 cm	30 cm

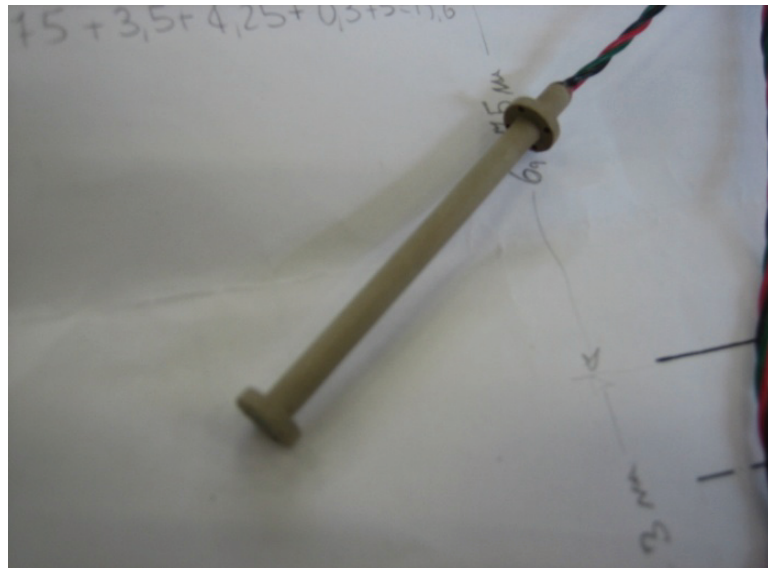


Figure 15: Luchsinger strain-gauge for embedment in concrete

The taxiway concrete (rehabilitated) and flexible (non-rehabilitated) pavements share the same subbase, subgrade and wearing courses (Tab. 1). In the concrete pavement, the base and binder courses were replaced by a slab of plain concrete, in the first section, and rubberized concrete, in the second section (Fig. 14). To the author's knowledge, this is the first time that rubberized concrete is used in airfield pavements. It is also the first time that rubberized concrete is used for testing full-scale structural elements. The present experimentation follows many years of laboratory investigations on rubberized concrete specimens, performed at the LISG laboratory of the Engineering Faculty of Bologna. The main finding of these preliminary investigations is that rubberized concrete works better than plain concrete during fatigue cycles, delaying cracking and crushing. Since fatigue is one of the main causes of distress in pavements, this finding is the reason why the authors have proposed the use of rubberized concrete in airfield pavements, where the repetition is lower but the intensity of loads is greater than in highway pavements. Actually, as is well known, the number of fatigue cycles a material can bear before crushing decreases with increasing applied loads.

The plain concrete section of the experimentation has been carried out for comparison purposes, so that we could evaluate how the pavement performance is affected by rubberization. The thicknesses of the several layers of the three pavements (the two of the experimentation and the non-rehabilitated one) are collected in Tab. 1.

Note how the thickness of the concrete slab (16 cm) is about one third the slab thickness of a rigid pavement for taxiways ($40 - 50\text{ cm}$), both for Section 1 and 2. For this reason, the pavement we have built cannot be classified as rigid in a strict sense, even if it is a concrete pavement. We cannot expect it to behave like a rigid beam. It is rather a semi-rigid pavement, with some degree of deflection allowed and a mechanism of stress transfer that is intermediate between those showed in Figs. 4 and 9. This is especially true for the rubberized section, since rubberization dramatically reduces the strength of concrete.

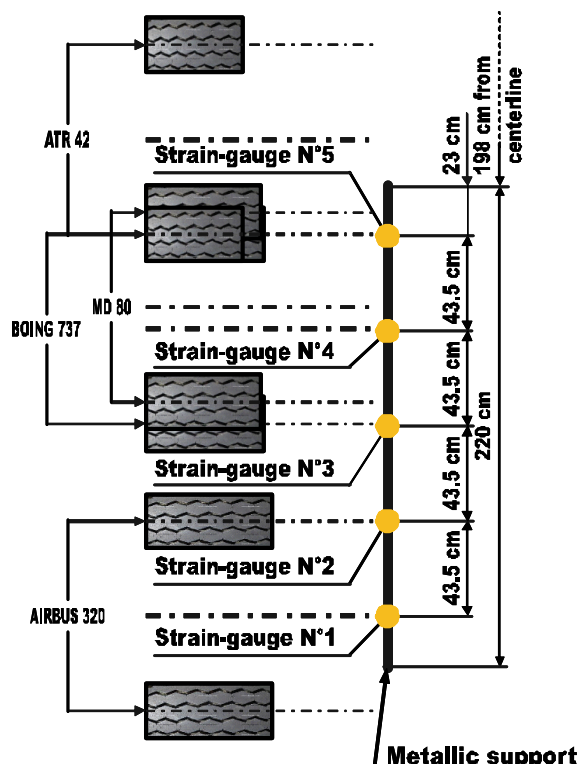


Figure 16: Detail of the metallic support and relative positions of the strain gauges to the wheels of the aircrafts covering 74% of the annual traffic

The two sections were instrumented with strain gauges embedded in concrete (Fig. 15). The strain gauges were positioned along two transverse sections, one for each section of the semi-rigid pavement (Fig. 14), so as to acquire the vertical strains due to the wheel loads. Only one half of each transverse section was instrumented (Fig. 14). The strain gauges were positioned just below the upper bound of the concrete slabs.

As previously said (§2), the taxiway is an area of highly channelized traffic, due to its low wander width. This configures the taxiway as an optimum area for the experimental analysis of the distresses due to repeated loads. Moreover, the high channelization allowed us to identify with a good degree of precision the transverse gear wheel locations for the aircrafts landing at the Guglielmo Marconi airport. It was found that five equally spaced locations covers 74% of the annual airport traffic (Tab. 2). They are spaced for intervals of 43.5 cm (Fig. 16), with a distance of 221 cm between the centre line and the closer location.



Figure 17: Positioning of the strain gauges over the metallic support



Figure 18: Concreting of Section 2 semi-rigid pavement



Figure 19: Concrete flowing through the strain-gauges during concreting

Fig 17 shows five of the ten used strain gauges (five for each sections), settled out to be embedded under the five equally spaced lanes. The strain gauges were connected

to a real-time controller, which also allows for remote data acquisition. Fig. 17 also shows the metallic support of the strain gauges, which has been fixed to the subbase course to allow the strain-gauges to maintain the correct position during concreting (Figs. 18, 19).

4 Mix-design and properties of the fresh concrete

The two concrete mixtures used in the experimentation share the same type of binder (Portland II AL 45.5R Micronmineral), alluvial coarse aggregates ($8 - 15\text{ mm}$) and fine aggregates (sand of $0 - 5\text{ mm}$ and Po sand of $0 - 2\text{ mm}$).

A finer kind of fine aggregates, Po sand, was added to sand since the gradation analysis of the employed sand had shown a poor content of fine fractions. This follows in a high Fineness Modulus (FM) of fine aggregates when only sand is used. Fineness Modulus is an empirical number relating to the fineness of the aggregate, used in determining the degree of uniformity of the aggregate gradation. The derivation of this parameter was based on the use of a single parameter to describe a grading curve. The higher the FM , the coarser the aggregate. The fineness Modulus is defined as the sum of the cumulative percentages retained on specified sieves divided by 100:

$$FM = \frac{\text{cumulative percentage retained on specified sieves}}{100}. \quad (5)$$

In the literature, several authors suggest the derivation of Fineness Moduli. They all vary between one another regarding their derivation. Well-known examples of such measures are the FM obtained by Abrams [Abrams (1918a); Abrams (1918b)], Faury's "l'indice pondéral" [Faury (1958)], the F-value obtained by Hummel [Hummel (1959)], Spindel's R-value or the "Kornpotenz" (grain power) obtained by Stern [Stern (1932)]. The latter all being variants of Abrams' FM . According to EN 12620, sand FM is calculated here as the summation of the oversize material (in Vol.-%) of the 4 mm , 2 mm , 1 mm , 0.5 mm , 0.25 mm and 0.125 mm sieves divided by 100:

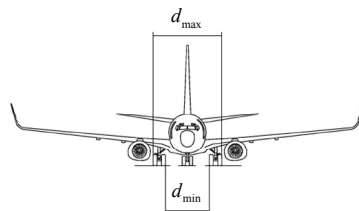
$$FM = \frac{\Sigma \{(> 4) + (> 2) + (> 1) + (> 0.5) + (> 0.25) + (> 0.125)\}}{100} = 3.52. \quad (6)$$

The value given by Eq. (6) is high due to the poor sand content passing the 0.25 mm and 0.125 mm sieves. Moreover, sand gradation does not fulfill the ASTM requirement of having $10 - 30\%$ passing the 0.3 mm sieve and $2 - 10\%$ passing the 0.15 mm sieve, following in a grading curve that slightly outgoes the ASTM upper bound limit curve (ASTM C 33-71 a).

Po sand is a very fine monogranular aggregate ($FM = 1.97$) with 85% of the gradation included between 0.1 mm and 1 mm . In order to decrease the cumulative FM of natural fine aggregates in the rubberized mixture, sand was mixed in 79.5 Vol.-% (ssd) with Po sand for the remaining 20.5 Vol.-% (ssd). Adding Po sand leads to a fine aggregate gradation with 18% passing the 0.3 mm sieve and 5% passing the 0.15 mm sieve. Moreover, the cumulative grading curve of fine aggregates lies between the two ASTM limit bound curves.

In the control mixture, a percentage of 85.4 Vol.-% (ssd) of sand and 14.6 Vol.-% (ssd) of Po sand was sufficient to fulfill ASTM requirements.

Table 2: Percentage annual traffic and track widths for the aircrafts most frequently landing at Bologna



Aircraft	Annual traffic [%]	d_{\max} (Max track width) [cm]	d_{\min} (Min track width) [cm]
BOEING 737	28.9	641	399
AIRBUS 320	18.3	902	678
CRJ	10	400	176
ATR 42	8.5	467	243
MD 80	8.3	621	397

The rubber aggregates were obtained by mechanical grinding of tires, without any kind of purification. Therefore, they may contain small amounts of steel and textile fibers. According to previous studies [Bignozzi and Sandrolini (2004); Bignozzi and Sandrolini (2005)], aiming at evaluating the optimum amount of tire rubber that can be substituted to sand thus avoiding severe loss of compressive strength, we chose here to use a 22 Vol.-% substitution percentage. The rubber aggregates were replaced with sand since it was found [Bignozzi and Sandrolini (2004); Bignozzi and Sandrolini (2005)] that the best results for workability and mechanical strength were obtained when the sand fraction, and not the fine filler fraction, was replaced by waste tire of similar grain size. A $1 - 2.4\text{ mm}$ rubber aggregate was used here.

Once we defined the fine aggregate composition, the amount of coarse aggregate was computed according to the Füller grain size distribution. The cumulative aggregate FM (coarse aggregates + fine aggregates) for rubberized concrete is equal to 5.22.

In the following, the control and the rubberized mixture will be named Mixture 1 and Mixture 2, respectively. The aggregate composition of the two mixtures is shown in Tab. 3, where all the percentages are computed in the assumption of saturated surface dry condition (ssd).

Coarse and fine natural aggregates and rubber aggregates (only for Mixture 2) were fed into the concrete mixer in the order and mixed for 5 min. The cement was then added and mixed with aggregates for 2 min. more. Finally, 75% of the water and the admixture with the remaining water were added and mixed for 10 min.

The workability of the fresh concrete was assessed with the Abrams slump test, performed in compliance with UNI 9418 and UNI EN 12350-2. For both mixtures, the desired consistency of fresh concrete was the S5 consistency class, the super fluid class (UNI EN 206-1:2006, UNI 11104:2004), with a target slump of $220 \pm 30 \text{ mm}$ (according to UNI EN 206-1:2006, the tolerance applied to a target slump $\geq 100 \text{ mm}$ is $\pm 30 \text{ mm}$). To reach a super fluid consistency, a considerable amount of water is required. This leads to a decrease in strength and resistance to frost and aggressive environments in hardened concrete and to an increased danger of segregation and bleeding. In order to reach a super fluid consistency without exceed in quantity of water, we have used a polyacrylic superplasticizer admixture (Axim Creative LX fluxing agent) for an amount of 0.65% in relation to the cement mass in Mixture 1 and 0.8% in Mixture 2. This allowed a water reduction by 16% for Mixture 1 and 21% for Mixture 2. The slump was 220 mm for Mixture 1 and 215 mm for Mixture 2, matching the target slump in both cases.

5 Experimental results

5.1 Laboratory tests on hardened concrete

According to UNI EN 206-1:2006, the hardened concrete is classified on the basis of the value assumed by ρ , the volumic mass or density, after oven-drying (EN 12390-7):

- Light-weight concrete, if ρ ranges between 800 and 2000 kg/m^3 ;
- Normal-weight concrete, if ρ ranges between 2000 and 2600 kg/m^3 ;
- Heavy-weight concrete, if ρ is greater than 2600 kg/m^3 .

The oven-dry density of Mixture 2, computed as mean value evaluated on two cubic specimens of 15 cm side each, is intermediate between that of a normal- and light-weight concrete:

$$\rho = 1976 \text{ kg/m}^3, \quad (7)$$

Table 3: Aggregate composition in saturated surface dry condition (ssd)

	Mixture 1		Mixture 2	
	Weight%	Volume%	Weight%	Volume%
Coarse aggregates	51.9%	52.0%	53.1%	50.0%
Sand	41.0%	41.0%	33.0%	31.0%
Po sand	7.1%	7.0%	8.6%	8.0%
PFU	/	/	5.3%	11.0%

Table 4: Mechanical properties of Mixture 1 and 2 after 28 day curing (UNI 6126, UNI 6127, UNI 6130/I, UNI 6130/II, UNI 6132, UNI 6556:1976).

Mixture 1		Mixture 2	
Compressive strength [N/mm ²]	Elastic modulus [N/mm ²]	Compressive strength [N/mm ²]	Elastic modulus [N/mm ²]
56.07	13573	20.95	7340

with a water absorption by immersion (EN 1097-6, UNI 7699), expressed as the water uptake relative to the oven-dry mass, equal to:

$$W = \frac{M_{ssd} - M_{dry}}{M_{dry}} = 7.62\%, \quad (8)$$

where M_{ssd} is the saturated surface dry mass and M_{dry} is the oven-dry mass. The value provided by Eq. (8) is slightly smaller than the water absorption by immersion of Mixture 1.

The specimens used for uniaxial compression tests were cylinders of 15 cm (diameter) × 30 cm (high). After uniaxial compression test, the specimens prepared with

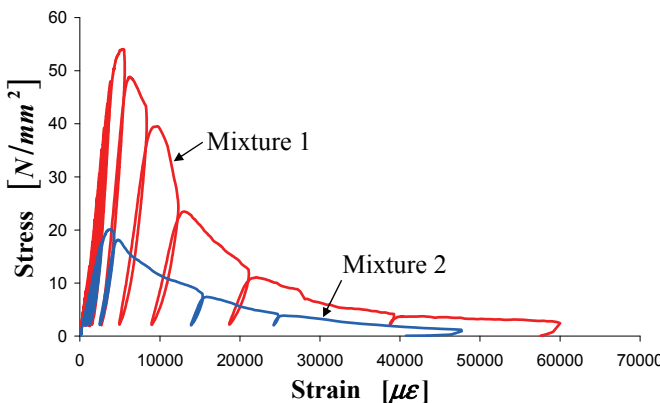


Figure 20: Stress-strain relationships for the two mixtures after 28 day curing

Mixture 2 appeared to have a very good distribution of the rubber aggregates in the cement paste and did not show any signs of segregation.

Fig. 20 shows the stress-strain relationships for two specimens prepared with Mixture 1 and 2, respectively. The 28 days mean compressive strengths and elastic modules for Mixture 1 and 2 (averaged over 3 specimens) are collected in Tab. 4. The decrease in compressive strength when the rubber is added is well evident from both Fig. 20 and Tab. 4. Nevertheless, it is not essential for airfield applications, since the loads carried by airfield pavements are very far from the collapse load and led the concrete to work in linear-elastic field in both experimental sections (stresses do not exceed 0.16 N/mm^2). Consequently, there are no unrecovered strains that cumulate for cyclic loads even when the rubber is added to concrete. This is an important requirement for airfield pavements, since it is as much essential to delay fatigue cracking as to avoid high surface deformation before failure, which may cause discomfort to passengers or high stresses in the plane (functional failure, §2). We can thus conclude that the 22 Vol.-% rubberization does not excessively weaken the concrete compressive strength and the pavement preserves a good safety factor as far as the failure load is concerned. Moreover, the rubberized concrete does not lead to accumulated plastic strains in airfield pavements, even if it possesses a plastic energy higher than that of plain concrete.

In Fig. 20 we can also appreciate how the slope of the unloading-reloading cycles is lower for Mixture 2 than for Mixture 1. This means that the elastic strain is recovered faster for Mixture 2 than for Mixture 1 when unloading after the elastic range. Nevertheless, the recovered (elastic) strain is bigger for Mixture 1 than for Mixture 2 for any prefixed value of unloading strain, due to the combined effect of

a lower length of unloading and a lower stress of unloading for Mixture 2.

The elastic modulus of the wearing course, which is bitumen, is of the order of $3 \cdot 10^3 N/mm^2$. This value is smaller than the elastic modulus of concrete, both plain and rubberized (Tab. 4). It is worth noting that the mismatch between the elastic modules of Mixture 2 and bitumen (Section 2) is smaller than the mismatch between the elastic modules of Mixture 1 and bitumen (Section 1). In the plane deformed sections assumption, which is here applicable, the mismatch between elastic modules involves an interfacial discontinuity in stress, which is smaller in Section 2 than in Section 1, at the tack coat (Fig. 4). This means that Section 2 is preserved against interfacial failure better than Section 1.

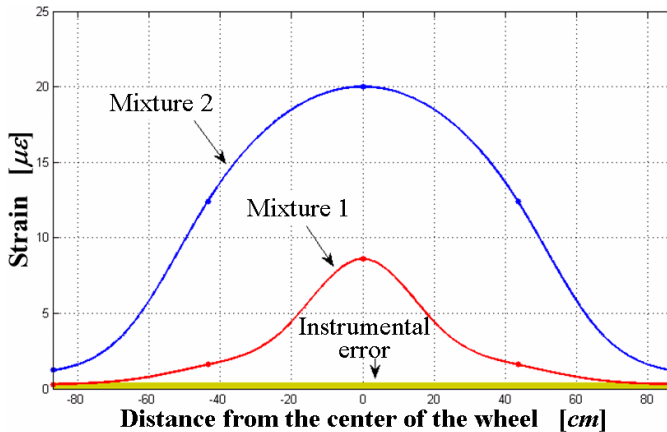


Figure 21: Acquired data and interpolation curves for the strains in plain and rubberized concrete

5.2 *In-situ acquired data and discussion*

Results concerning the strain and stress profiles along the two instrumented cross-sections when the gear wheels stand over them are presented here. The two curves in Fig. 21 interpolate the strains acquired on the two cross-sections. The strain curve of Mixture 2 is smoother than that of Mixture 1. This behavior and the peak strain greater for Mixture 2 than for Mixture 1 imply that strains are spread over a greater area and strain curves of different airfields overlap on a greater portion for Mixture 2 as compared with Mixture 1. The consequence is an improvement of the rutting performance of concrete pavements. In fact, we have previously discussed (§5.1) how both concrete sections work in linear-elastic field. This makes the problem of the traffic lanes created by individual lateral wander patterns (§2)

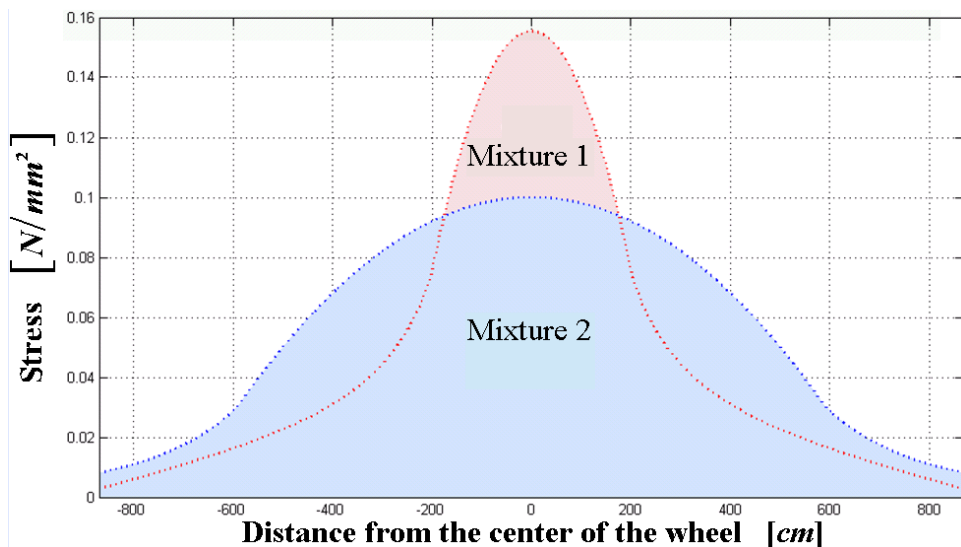


Figure 22: Identified stresses in plain and rubberized concrete

inessential, since the lanes are a consequence of the accumulation of plastic (inelastic) strains for cyclic loads. Nevertheless, we must remember that the linear-elastic field is only a schematization of a more complex material behavior and very small plastic strains occur even for very small applied loads. With this in mind, Fig. 21 allows us to state that, if small plastic strains arise in the pavements, they are less effective in creating traffic lanes in rubberized than in plain concrete pavement.

The stress curves for the two mixtures (Fig. 22) have been obtained in the first-order approximated uniaxial assumption:

$$\sigma = E \varepsilon, \quad (9)$$

where E is the Young modulus (Tab. 4).

It is worth noting that the curves in Fig. 22 provide the vertical stress field on the upper bound of the concrete slab, where the strain-gauges are positioned. For this reason, they cannot be compared to the schemes of stress transfer in Figs. 4 and 9, both providing the vertical stress field at a greater depth, in the base course. Consequently, the curves in Fig. 22 are not useful for clarifying how close the behavior of the semi-rigid pavement is to the flexible rather than rigid scheme.

While strains are higher for Mixture 2 than for Mixture 1, when identifying the cross-sections stresses we find that the peak stress is lower in Mixture 2 than in Mixture 1 (Fig. 22). This happens since k_E , the ratio between E_2 , the elastic mod-

ulus of Mixture 2, and E_1 , the elastic modulus of Mixture 1:

$$k_E = \frac{E_2}{E_1}, \quad (10)$$

is lower than k_ε , the ratio between the peak strains of Mixture 1 and 2, ε_1 and ε_2 respectively:

$$k_\varepsilon = \frac{\varepsilon_1}{\varepsilon_2}. \quad (11)$$

Consequently:

$$\sigma_2 = E_2 \varepsilon_2 = k_E E_1 \varepsilon_2 = \frac{k_E}{k_\varepsilon} E_1 \varepsilon_1 = \frac{k_E}{k_\varepsilon} \sigma_1 < \sigma_1, \quad (12)$$

where σ_1 is the peak stress in Mixture 1, σ_2 is the peak stress in Mixture 2, and

$$k_E < k_\varepsilon \Rightarrow \frac{k_E}{k_\varepsilon} < 1. \quad (13)$$

One of the main consequences of having $\sigma_2 < \sigma_1$ is that the stress field depends on the elastic properties of the mixture (Young's and Poisson's modules). This is a remarkable result, since it contradicts Boussinesq's closed form solution for a homogeneous, linear-elastic, and isotropic half-space subjected to a point-load perpendicular to the surface. Actually, Boussinesq's vertical stress (Eq. (1)) depends on distance r between the application and the evaluation points and angle θ between the point load vector and the radial arm connecting the application to the evaluation point only. Neither in Fröhlich's equation (Eq. (2)) the vertical stress is an explicit function of the elastic modules.

A dependence of the stress field on the elastic properties was also found by Olmstead and Fischer (2009), who compared the values given by Fröhlich's equation with the experimental values obtained from pressure pads embedded in sand, wet sand, and silt, carried by a single wheel. They measured vertical stresses depending on the soil type, while Fröhlich's value did not change except for the change in depth. On the other hand, the experimental results were also validated from a physical point of view, since it seems very strange that the way the stresses spread through the medium does not depend on the elastic parameters of the medium itself. Moreover, it must be pointed out that Boussinesq's theory was shown to be poor in providing stresses and deflections (§2.3), which were found to be greater than measured values, particularly near the surface. This may explain the discrepancy between Boussinesq's predictions and acquired values, since the strain-gauges were embedded near the upper bound of the concrete slab.

In conclusion, it seems that Boussinesq's theory and all the theories derived from it, included Fröhlich's, must be revised as far as the predicted behavior of stresses near the surface is concerned. Moreover, since Fröhlich's equation gives the classic CBR (California Bearing Ratio,) equation for $n = 2$ (§2.3), all the uncertainties over Fröhlich's equation can be extended to the CBR equation. This may explain many of the well-known deficiencies of the CBR method. In particular, the overestimation of deflection by Boussinesq's and related methods may explain the overestimation of deflection by the CBR method and the need to introduce corrective alpha factors for the thickness design of pavements.

Fig. 22 shows that the lower maximum stress achieved in Mixture 2 gives rise to a stress curve smoother than that of Mixture 1. This follows in lower stress gradients for Mixture 2 than for Mixture 1. Since a high stress gradient is one of the main causes of distress for repeated loads, it is reasonable to expect a longer economic life for Mixture 2 than for Mixture 1.

Moreover, the two curves in Fig. 22 intersect, following in a greater stressed area when Mixture 2 is used instead of Mixture 1. This behavior fulfils the vertical equilibrium requirement. Actually, the area below the two curves must be the same, since this area gives the applied load, equal in both cases. The difference between the two areas in Fig. 22 is negligible if we consider the error introduced in approximating the triaxial state of stress with a uniaxial one (Eq. 9) and the further error due to a finite extension of the instrumented field, smaller than the stressed field.

The conservation of equilibrium gives validity to the identified data and the related discussions, including that on Boussinesq's theory.

6 Conclusions

The new type of airfield pavement proposed here is an intermediate solution between a flexible and a rigid pavement. A rubberized cement concrete mixture has been used for preparing a concrete slab customarily used for rigid pavements, but the subbase and subgrade courses were those typical of a flexible pavement and the concrete slab thickness was much smaller than that of a rigid pavement. The experimental results were compared with those of a control plain concrete mixture that differed from the previous in the concrete mixture only. Due to the small thickness, neither the rubberized nor the control slab worked as a rigid pavement and the stresses were not uniformly transmitted to the soil. This implies that Westergaard's theory cannot be employed for modeling this type of concrete slabs. The value of aircraft-induced stress is more likely to be achieved by means of layered elastic analysis.

The in-situ real-scale experimentation showed that rubberized concrete is more ef-

fective than plain concrete in spreading the applied load and distributing it over a large area of the concrete slab/subbase course interface. Since a larger stressed area involves a lower mean stress, this means that the subbase works at lower levels of stress with a rubberized rather than a plain concrete slab over it. This allows us to better exploit the strength properties of the subbase course and brings about economic benefits when a rubberized slab is used instead of a plain concrete slab. It is worth noting how the rubberization of concrete by means of waste tires is an attractive technique not only for the economic benefits connected to the structural performance presented here, but also for the environmental problem related to the recycling of waste tires. As far as this last point is concerned, a number of techniques have been proposed in the past for recycling waste tires and allow for their reuse in non-structural elements. The novelty of this study is that, for the first time, the recycling was focused on the obtainment of structural elements. The experimentation showed that this is possible and, in particular cases, such as that of airfield pavements, also may lead to more convenient applications than traditional ones.

The experimental results also exhibit a dependence of the vertical stresses on the elastic properties of the concrete slab, which is not accounted by neither Boussinesq's findings nor the modified closed solutions of the elastic problem in half-spaces subjected to a point load. This important result has been achieved by using strain-gauges embedded in concrete, which allowed for the first time comparison between the experimental data acquired in plain and rubberized concrete. Since the experimental results seem to be reliable, due to the fact that they satisfy equilibrium, this indicates that Boussinesq's elastic solution must be carefully revised [Ferretti, in preparation], looking for a higher order solution that also allows us to evaluate the role played by the Young's and Poisson's modules.

7 Future developments

The revision of Boussinesq's closed elastic solution suggested by this experimentation may lead to a better comprehension of the stress field induced by an aircraft to the airfield pavements. In particular, it may clarify the mechanism of stress transfer near the surface for static and dynamic loads, that seems not to be sufficiently exploited at present. In perspective, the enhanced theory of Boussinesq may lead to formulate a more realistic criterion of design for airfield pavements, which better accounts for stresses and deflections than the methods currently used.

Acknowledgement: The staff of SAB – infrastructures development, Guglielmo Marconi Airport of Bologna (Italy), and, in special way, Domenico Terra, Engineer, are gratefully acknowledged for having assigned the taxiway of the airport to the

experimentation of the new proposed airfield pavement.

References

- Abrams, D.A.** (1918a): The basic principles of concrete mixes. *Mining and Scientific Press*, pp. 23–24.
- Abrams, D.A.** (1918b): *Design of Concrete Mixtures*. Bulletin 1, Structural Materials Research Laboratory, Lewis Institute, Chicago, pp. 1–22.
- Barker, W.R., Gonzalez, C.R.** (2006): *Independent Evaluation of 6-Wheel Alpha Factor Report*. Letter Report to the Federal Aviation Administration, U.S. Army Engineer Research and Development Center, Vicksburg, Mississippi.
- Bennet, D.** (2004): Airfield Pavement Surface Evaluation and Rating Manuals. *Advisory Circular*, U.S. Department of Transportation, Federal Aviation Administration.
- Binger, R.L., Wells, L.G.** (1989): *Simulation of compaction from surface mining systems*. ASAE Paper no. 89-2018, St. Joseph, MI: ASAE.
- Bignozzi, M.C., Sandrolini, F.** (2004): Recycling tyre rubber in building materials. Proc. *International Conference: Sustainable Waste Management and Recycling: Used/Post-Consumer Tyres*, Kingston University, London, September 14–15 2004, Thomas Telford, London, pp. 77–84.
- Bignozzi, M.C., Sandrolini, F.** (2005): Il riciclo di pneumatici particellati come aggregati fini in malte cementizie auto compattanti. Proc. *Seminari di Ecomondo 2005*, Maggioli Editore, 26-29 Ottobre 2005, Rimini, pp. 41–46.
- Bignozzi, M.C., Sandrolini, F.** (2006): Tyre rubber waste recycling in self-compacting concrete. *Cement Concrete Res.*, vol. 36, pp. 735–739.
- Boussinesq, M.J.** (1876): *Essai théorique sur l'équilibre d'élasticité des massifs pulvérulents comparé à celui de massifs solides et sur la poussée des terres sans cohésion*. Mémoires des Savants Etrangers, Académie de Belgique, 40, Bruxelles.
- Boussinesq, M.J.** (1885): *Application des potentiels à l'étude de l'équilibre et du mouvement des solides élastiques, avec des notes étendues sur divers points de physique mathématique et d'analyse*. Gauthier-Villars imprimeur libraire, Paris.
- Burmister, D. M.** (1943): The Theory of Stresses and Displacements in Layered Systems and Applications to the Design of Airport Runways. Proc. *Highway Research Board*, vol. 23.
- Caron, C., Theillout, J.N., Brill, D.R.** (2010): Comparison of US and French Rational Procedures for the Design of Flexible Airfield Pavements. Proc. *2010 FAA Worldwide Airport Technology Transfer Conference*, Atlantic City, New Jersey, USA, April 2010, 23 pp.

- Fattuhi, N.I., Clark, L.A.** (1996): Cement-based materials containing shredded scrap truck tyre rubber. *Constr. Build. Mater.*, vol. 10, no. 4, pp. 229–236.
- Faury, J.** (1958): *Le béton: influence des constituants inertes. Règles à adopter pour sa meilleure composition, sa confection et son transport sur les chantiers, Etudes de synthèse et de documentation*. Dunod, Paris,.
- Fedroff, D., Ahmad, S., Savas, B.Z.** (1996): Mechanical properties of concrete with ground waste tire rubber. *Transportation Research Board 1996; Report No. 1532*, pp. 66–72.
- Ferretti, E.** (under preparation): A Higher Order Solution of the Elastic Problem of Boussinesq for an Homogeneous, Linear-Elastic, and Isotropic Half-Space Subjected to a Point Load.
- Fröhlich, O.K.** (1934): *Druckverteilung im Baugrunde*. Springer Verlag, Wien.
- Ghaly, A.M., Cahill IV, J.D.** (2005): Correlation of strength, rubber content, and water to cement ratio in rubberized concrete. *Can. J. Civil. Eng.*, vol. 32, no. 6, pp. 1075–1081.
- Gonzales, C.R.** (2006): Implementation of a New Flexible Pavement Design Procedure for U.S. Military Airports. Proc. *Fourth LACCEI International Latin American and Caribbean Conference for Engineering and Technology* (LACCEI'2006), Mayagüez, Puerto Rico, 21-23 June 2006, 2006, 10 pp.
- Hernandez-Olivares, F., Barluenga, G., Bollatib, M., Witoszek, B.** (2002): Static and dynamic behaviour of recycled tyre rubber-filled concrete. *Cement Concrete Res.*, vol. 32, no. 10, pp. 1587–1596.
- Ho Sang, V.A.** (1975): Field survey and analysis of aircraft distribution on airport pavements. Report No. FAA-RD-74-36. U.S. Federal Aviation Administration.
- Hummel, A.** (1959): *Das Beton-ABC – Ein Lehrbuch der Technologie des Schwerbetons und des Leichtbetons*. 11th edn, Wilhelm Ernst & Sohn, Berlin.
- Khatib, Z.K., Bayomy, F.M.** (1999): Rubberized Portland cement concrete. *J. Mater. Civil. Eng.*, vol. 11, no. 3, pp. 206–213.
- Kringos, N., Scarpas, A., Selvadurai, A.P.S.** (2008): Simulation of Mastic Erosion from Open-Graded Asphalt Mixes Using a Hybrid Lagrangian-Eulerian Finite Element Approach. *CMES: Computer Modeling in Engineering & Sciences*, vol. 28, no. 3 pp. 147–159.
- Kwon, S.H., Lee, H.K.** (2009): A Computational Approach to Investigate Electromagnetic Shielding Effectiveness of Steel Fiber-Reinforced Mortar. *CMC: Comput. Mater. Con.*, vol. 12, no. 3, pp. 197–221.
- Lee, B.Y., Kim, J.K., Kim, J.S., Kim, Y.Y.** (2009): Quantitative evaluation technique of Polyvinyl Alcohol (PVA) fiber dispersion in engineered cementitious com-

posites. *Cement Concrete Comp.*, vol. 31, no.6, pp. 408–417.

Lee, B.Y., Lee, Y., Kim, J.K., Kim, Y.Y. (2010): Micromechanics-Based Fiber-Bridging Analysis of Strain-Hardening Cementitious Composite Accounting for Fiber Distribution. *CMES: Computer Modeling in Engineering & Sciences*, vol. 61, no. 2 pp. 111–132.

Li, G.Q., Stubblefield, M.A., Gregory, G., Eggers, J., Abadie, C. and Huang, B.S. (2004): Development of waste tire modified concrete. *Cement Concrete Res.*, vol. 34, no. 12, pp. 2283–2289.

Manzanal, D., Pastor, M., Merodo J.A.F., Mira, P. (2010): A State Parameter Based Generalized Plasticity Model for Unsaturated Soils. *CMES: Computer Modeling in Engineering & Sciences*, vol. 55, no. 3, pp. 293–317.

Naik, T.R., Siddique, R. (2004): Properties of concrete containing scrap tire rubber – an overview. *Waste Manage*, vol. 24, no. 6, pp. 563–569.

Odemark, N. (1949): *Undersökning av elasticitetegenskaperna hos olika jordarter samt teori för beräkning av belägningar enligt elasticitetsteorin*. Statens Väginstitut, meddelande 77.

Olmstead, T., Fischer, E. (2009): *Estimating Vertical Stress on Soil Subjected to Vehicular Loading*. US Army Corps of Engineers, Engineer Research and Development Center, Cold Regions Research and Engineering Laboratory, ERDC/CRREL TR-09-02, Washington.

Packard, R.G. (1973): *Design of Concrete Airport Pavement*. Engineering Bulletin, Portland Cement Association, Skokie, Illinois.

Pahr, D.H., Böhm, H.J. (2008): Assessment of mixed uniform boundary conditions for predicting the mechanical behavior of elastic and inelastic discontinuously reinforced composites. *CMES: Computer Modeling in Engineering & Sciences*, vol. 34, pp. 117–136.

Pu, Y., Zhihai, X., Xiasong, H., Guorong, L., Haili, Z., Xiaoqin, M. and Zhangzhi, C. (2009): Limit Load of Soil-Root Composites. *CMC: Comput. Mater. Con.*, vol. 10, no. 2, pp. 117–137.

Pyo, S.H., Lee, H.K. (2009): Micromechanical analysis of aligned and randomly oriented whisker-/ short fiber-reinforced composites. *CMES: Computer Modeling in Engineering & Sciences*, vol. 40, pp. 271–305.

Selvadurai, A.P.S., Ghiabi, H. (2008): Consolidation of a Soft Clay Composite: Experimental Results and Computational Estimates. *CMES: Computer Modeling in Engineering & Sciences*, vol. 23, no. 1, pp. 53–73.

Seyrafian, S., Gatmiri, B., Noorzad, A. (2007): Analytical Investigation of Depth Non-homogeneity Effect on the Dynamic Stiffness of Shallow Foundations. *CMES*:

- Computer Modeling in Engineering & Sciences*, vol. 21, no. 3, pp. 209–217.
- Sharifat, K., Kushwaha, R. L.** (2000): *Modeling soil movement by tillage tools*. Saskatoon, Saskatchewan Canada: Department of Agricultural and Bioresource Engineering, University of Saskatchewan.
- Söehne, W.** (1958): Fundamentals of pressure distribution and soil compaction under tractor tires. *Agricultural Engineering*, vol. 39, pp. 276–281.
- Stern, O.** (1932): Vorschlag für eine Norm: Kornpotenz (Feinheitsmodul) loser Haufwerke. *Sparwirtschaft*, 4, in German.
- Topçu, İ.B.** (1995): The properties of rubberized concretes. *Cement Concrete Res.*, vol. 25, no. 2, pp. 304–310.
- Topçu, İ.B., Sarıdemir, M.** (2008): Prediction of rubberized concrete properties using artificial neural network and fuzzy logic. *Construction Build. Mater.*, vol. 22, pp. 532–540.
- Ververka, V.** (1973): *Modules, contraintes et déformations des massifs et couches granulaires*. Rapport de Recherche, no. 162, vv, Centre de Recherches Routières, Bruxelles.
- Wang, Y., Wu, H.C., Li, V.C.** (2000): Concrete reinforcement with recycled fibers. *J. Mater. Civil. Eng.*, vol. 12, no. 4, pp. 314–319.
- Wei, V.N.Y.** (2009): *The development of airside infrastructure at the Senai International Airport: a case study*. PhD thesis, Faculty of Civil Engineering, Universiti Teknologi Malaysia.
- Westergaard, H.M.** (1943): New Formulas for Stresses in Concrete Pavements of Airfields. *ACE Transactions*, vol. 108. Also in *ACE Proceedings*, vol. 73, no. 5, May, 1947.
- Yang, H.S., Kim, D.J., Lee, Y.K., Kim, H.J., Jeon, J.Y., Kang, C.W.** (2004): Possibility of using waste tire composites reinforced with rice straw as construction materials. *Bioresource Technol.*, vol. 95, pp. 61–65.
- Yoder, E.J., and Witczak, M.W.** (1975): *Principles of pavement design*. John Wiley & Sons, Inc., New York.
- Zheng, L., Sharon Huo, X., Yuan, Y.** (2008): Experimental investigation on dynamic properties of rubberized concrete. *Constr. Build. Mater.*, vol. 22, pp. 939–947.

